ARTICLE TEMPLATE

Interval Sliding Mode Observer based Fault Accommodation for Non-minimum Phase LPV Systems with Online Control Allocation

Kangkang Zhang[a,b], Bin Jiang[a], Xinggang Yan[b] and Christopher Edwards[c]

[a]College of Automation Engineering, Nanjing University of Aeronautics and Astronautics, Nanjing210016, China;
[b]School of Engineering and Digital Arts, University of Kent, Canterbury, Kent CT2 7NT, United Kingdom;
[c] College of Engineering, Mathematics, and Physical Sciences, University of Exeter, Exeter, EX4 4QF, United Kingdom.

ARTICLE HISTORY
Compiled October 29, 2019

ABSTRACT
This paper proposes an interval sliding mode observer (ISMO) based sliding mode actuator fault accommodation (FA) framework for non-minimum phase linear-parameter-varying (LPV) systems involving online control allocation (CA) problem. Firstly, a specifically designed coordinate transformation is introduced to deal with the non-minimum phase issue. Then, for the transformed system, an ISMO is proposed to estimate the set of admissible values for the states of the faulty LPV systems. It is constructed based on the designed interval bounds for the scheduling-parameter-related uncertainties and fault-related items. The observer is designed by combining the interval observer and the sliding mode observer techniques. A fault-tolerant control (FTC) law with an online CA scheme is subsequently designed by stabilizing the proposed ISMO instead of the original faulty LPV system, which guarantees that the unmeasurable states of the original LPV system converge to zero asymptotically, the measurable outputs converge to zero in finite time, and further, the actual control efforts are allocated to all actuators optimally and satisfy prescribed performance. Finally, a simulation based on the inverter used in China Railway High-speed (CRH) is presented to illustrate the effectiveness of the proposed framework.

KEYWORDS
Sliding mode, interval observer, fault-tolerant control, control allocation

1. Introduction

In modern complex control systems, component faults may cause severe system performance degradation or, in the worst-case, may cause a break down of the entire system. In such situation, fault-tolerant control (FTC) aims to maintain the system performances close to the desired one or at least maintain the stability of the system. This is vital for critical systems such as aircraft, high-speed trains and nuclear power stations Zhang et al. (2012), Gao et al. (2015) in order to satisfy the increasing reliability and safety requirements. Generally speaking, FTC systems can be classified into two categories: *passive FTC systems* and *active FTC systems* Zhang et al. (2012). Passive

CONTACT Bin Jiang. Email: binjiang@nuaa.edu.cn

FTC systems are also called reliable control systems where FTC controllers are usually fixed and designed to tolerant specific anticipate faults. These schemes need neither fault diagnosis units nor controller reconfiguration. Active FTC systems on the other hand usually constructed based on information provided by fault detection and fault isolation (FDI) modules. As described in Jiang et al. (2006), fault accommodation (FA) (see Fan et al. (2017), Ye et al. (2006), Jiang et al. (2006) and Polycarpou (2001)) which concerns the faulty system, and system reconfiguration (SR) (see Tao et al. (2001), Ye et al. (2017) and Yang et al. (2010)) which focuses on the healthy (reconfigured) part of the system, are two effective ways to design active FTC systems. Fault detection and isolation for detecting the occurrence and locations of faults, and fault identification for determining the type and magnitude of faults are necessary for FA analysis and design. Actuator faults, including total and partial loss of effectiveness Boskovic et al. (2010), are a class of serious faults because they may damage the power units and control units which normally are the core entities of a system. Actuator FTC issues have been widely addressed in Boskovic et al. (2010), Tao et al. (2001), Tang et al. (2007), Alwi et al. (2008), Fan et al. (2017) and Ye et al. (2017) etc. In this paper, FA for actuator faults will be the main concern.

In FA, state observer design is the first step, which, however, is very challenging, especially for nonlinear systems. Linear-parameter-varying (LPV) representation introduced by Shamma (1988) provides an appealing alternative to replace the nonlinear complexity by an enlarged parametric variation, which may simplify the observer design. However, for the LPV system with unknown scheduling parameters, conventional observers such as Luenberger observers are not effective for estimation problems, while interval observers provide an alternative. The advantage is that interval observers provide the set of admissible of states instead of estimates generated by other observers such as Luenberger observers and Kalman filters. Interval observers, first proposed in Gouze et al. (2000) and further developed in Raïssi et al. (2010), Mazenc et al. (2011), Chebotarev et al. (2015) and Zheng et al. (2016) etc, have become an important observer for LPV systems. An interval observer has been proposed in Raïssi et al. (2010) for LPV representations to generate the admissible set of the states of one original nonlinear system using monotone system theory. The main restriction for interval observer design is to ensure the cooperativity of the interval estimation error dynamics. This has been overcome in Combastel (2013), Mazenc et al. (2011) and Raïssi et al. (2012) for linear time-invariant (LTI) systems, and Efimov et al. (2013) and Thabet et al. (2014) for linear time-varying (LTV) systems. Following the design trend of developing interval observers using monotone system theory, Chebotarev et al. (2015) proposed an approach to design interval observer for continuous-time LPV systems with an unmeasurable vector of scheduling parameters by considering L_1/L_2 performance, interval observers based on linear programming, and coordinate transformations proposed in Raïssi et al. (2012) and Efimov et al. (2013) are designed for nonnegative LPV systems, respectively, as well as ones based on Riccati matrix inequalities for generic LPV systems. For LPV systems with unknown scheduling parameters, it is necessary to consider the non-minimum phase cases. In Efimov et al. (2012), for the LPV systems with non-detectable or non-strongly-observable parts, an interval observer is designed using high order sliding mode techniques, which not only provides more accuracy setmembership estimates but also relaxes the applicability conditions of standard interval observer design method. However, only the structure of ISMO is presented in Efimov et al. (2012), the computation method for the designed gain matrix to deal with non-minimum phase issues is not specified. This paper will continue to research the ISMO design problem for non-minimum phase LPV systems

in terms of observer design step in FA.

In recent decades, the interest in FA for LPV systems has increased and many results have been published, for example Rotondo et al. (2014), Chen et al. (2017) and Sloth et al. (2010). But generally speaking, because conventional observers do not work well for estimating states and faults for general LPV systems, almost all of these results are developed for specific LPV systems under structure restrictions such as polytopic ones in Rotondo et al. (2014) or with measurable scheduling parameter (see e.g. Chen et al. (2017) and Sloth et al. (2010)). Recently, an effective methodology for controlling LPV systems with unknown scheduling parameters has been proposed based on interval observers in Efimov et al. (2013), which has subsequently been applied to FA for faulty LPV systems in Lamouchi et al. (2018). In traditional FA, the stability of the closed-loop system is guaranteed by achieving stability of both the estimation error system and the original faulty system. In the interval observer based FA approach, if the states of the interval observer for the original faulty system converge to zero, then the states of the original faulty system will converge to zero as well. Due to this advantage, in the interval observer based FA, if the states of the interval observer converge to zero, then the stability of the whole closed-loop FTC system can be guaranteed. Although the dimensions of interval observers are generally twice of those traditional observers such as Luenberger observers (see Efimov et al. (2013)), which may increase in making the states of the interval observer to converge to zero, interval observer based FA still provides an easier route in FTC design than traditional FA approaches because if the interval observer states converge to zero, then the states of both the estimation error system and the faulty system converge to zero. Unfortunately, there are very few results in terms of interval observer based FA except for Lamouchi et al. (2018), which motivates the work in this paper.

Since sliding mode observers are inherent robustness to matched uncertainties, sliding mode observer techniques have been introduced to interval observer design to generate tighter interval estimates. Except for Efimov et al. (2012), in Oubabas et al. (2018), an ISMO is constructed via a convex sum of an upper estimator and a lower estimator, while in Zhang et al. (2017), an ISMO is proposed based on regular form to detect incipient faults. On the other hand, sliding mode techniques have been used for FTC extensively because of their inherent robustness to matched uncertainties, for example, sliding mode FTC with online CA Alwi et al. (2008), Alwi et al. (2008) and Chen et al. (2017), and sliding mode observer based FTC Li et al. (2014) and Shi et al. (2015). However, to the best of the authors' knowledge, ISMOs have not been applied before to FA for LPV systems.

In this paper, an ISMO based sliding mode FA framework is proposed for non-minimum phase LPV systems with online CA for actuator loss of efficiency faults and outage faults. Specifically, the scheduling parameters may cause non-minimum phase issues for observable LPV systems. In this paper, this problem is addressed by introducing a new coordinate transformation satisfying a set of sufficient conditions. Proper interval bounds for scheduling-parameter-related uncertainties and fault-related items are induced, and an ISMO is proposed based on the interval bounds by combining interval observer and sliding mode observer techniques. A sliding mode FTC law is then designed, using the interval estimates generated by the proposed ISMO, to stabilize the ISMO by achieving the stability of the related sliding motion and the reachability. This in turn stabilizes the original LPV system. Finally, a simulation is presented to illustrate the effectiveness of the proposed FA. The main contribution of the proposed FA approach is summarized as follows:

- An ISMO is proposed for the faulty LPV systems by combining an interval observer and a sliding mode observer together to generate a tighter interval estimation than that produced by other interval observers which do not use sliding mode techniques.
- A sliding mode FTC law is designed to guarantee the convergence of the states of the ISMO instead of the states of the original faulty system, which can ensure that the unmeasurable states converge to zero asymptotically and the measurable states converge to zero in finite time. Furthermore, this approach is also applicable to some non-minimum phase LPV systems.

Notation : For two vectors $x_1, x_2 \in R^n$ or matrices $M_1,\ M_2 \in R^{m\times n}$, the relations $x_1 \leq x_2$ and $M_1 \leq M_2$ are understood elementwise. For any matrix $M \in R^{m\times n}$ and vector $x \in R^n$, $M^+ = \max\{0, M\}$, $M^- = \max\{0, -M\}$, $x^+ = \max\{0, x\}$ and $x^- = \max\{0, -x\}$. Denote by $|M|$ a $m \times n$ dimensional matrix with elements being the absolute values of the corresponding elements of M, and denote by $|x|$ a n dimensional vector with elements being the absolute values of the corresponding elements of x. The symbols M^+, M^-, x^+ and x^- are equivalently defined by $M^+ = \frac{1}{2}(M + |M|)$, $M^- = \frac{1}{2}(-M + |M|)$, $x^+ = \frac{1}{2}(x + |x|)$ and $x^- = \frac{1}{2}(-x + |x|)$, respectively. The notion $P \prec 0$ ($P \succ 0$) means that P is negative (positive) definite, and $P \preccurlyeq 0$ ($P \succcurlyeq 0$) means that P is nonnegative (nonpositive) definite. For $x_1, \cdots, x_n \in R$, $\mathrm{col}(x_1, \cdots, x_n)$ is a n dimensional column vector with elements $x_1, \cdots, x_n$. For $x = \mathrm{col}(x_1, \cdots, x_n) \in R^n$, $\mathrm{sign}(x) = \mathrm{col}(\mathrm{sign}(x_1) \cdots, \mathrm{sign}(x_n))$. The matrices I_n and E_n denote the identity matrix with dimension $n \times n$ and the matrix with all elements being 1 and dimension n.

2. Problem Formulation

Consider the LPV system similar to the ones in Lamouchi et al. (2018) and Efimov et al. (2013) as follows:

$$\dot{x} = Ax + \Delta A\left(\theta(t)\right)x + B_0(I_m - \rho)u, \tag{1}$$

$$y = Cx \tag{2}$$

where $x \in R^n$ is the state, $u \in R^m$ is the measurable control input and $y \in R^p$ is the measurable output. The matrices $A \in R^{n\times n}$ and $C \in R^{p\times n}$ are known with C being full row rank. The vector of scheduling parameters $\theta(t) \in \Pi$ is not available but the set $\Pi \subset R^h$ is known. The uncertain matrix $\Delta A\left(\cdot\right) : \Pi \longrightarrow R^{n\times n}$ is a piecewise continuous matrix function. It should be noted that the triple $(A + \Delta A(\theta(t)),\ B,\ C)$ may become non-minimum phase even if the triple $(A,\ B,\ C)$ is minimum phase because of $\Delta A\left(\cdot\right)$. Conditions in order to ensure minimum phase of the triple $(A + \Delta A(\theta(t)), B, C)$ in Alwi et al. (2012), Alwi et al. (2014) and Chen et al. (2017) will be removed in this paper.

The known matrix $B_0 \in R^{n\times m}$ is the actuator distribution matrix, which, in order to satisfy actuator redundancy condition that most of actuator FTC results with online CA scheme such as Alwi et al. (2008) and Chen et al. (2017) rely on, is assumed that $\mathrm{rank}(B_0) = q \leq m$. Then B_0 can be decomposed into a product of two full rank matrices $B_0 = BE$ where $B \in R^{n\times q}$ is full column rank, and $E \in R^{q\times m}$ is full row

rank. A *virtual control* v is then defined as

$$v = Eu \quad \Rightarrow \; B_0 u = Bv. \tag{3}$$

To simplify the notation and the exposition, only the case $p = q$ is considered in this paper. The result can be extended to the case $p \neq q$ easily.

The diagnose matrix $\rho = \text{diag}\{\rho_1, \cdots, \rho_m\}$ where $\rho_1, \cdots, \rho_m$ represent loss of efficiency factors. Note that ρ_i satisfies $0 \leq \underline{\rho}_i \leq \rho_i \leq \bar{\rho}_i \leq 1$ with $\underline{\rho}_i$ and $\bar{\rho}_i$ representing the lower bound and upper bound of ρ_i respectively. Thus, $0 \leq \underline{\rho} \leq \rho \leq \bar{\rho} \leq I_m$ where $\underline{\rho} = \text{diag}(\underline{\rho}_1, \cdots, \underline{\rho}_m)$ and $\bar{\rho} = \text{diag}(\bar{\rho}_1, \cdots, \bar{\rho}_m)$. It is worth pointing out that if $\underline{\rho}_i = \bar{\rho}_i = 1$, u_i has an outage fault and in the case $0 < \underline{\rho}_i \leq \bar{\rho}_i < 1$, u_i suffers from LOF, while $\underline{\rho}_i = \bar{\rho}_i = 0$ means that u_i is healthy. So in this paper, both outage faults and loss-of-effectiveness faults (LOFs) (see Ye et al. (2017) and Boskovic et al. (2010)) are considered.

In previous work for actuator FTCs (such as Tao et al. (2001), Chen et al. (2017) and Zhang et al. (2017)), actuator redundancy is necessary. Likewise here, the following similar assumption is required:

Assumption 2.1. The matrix $\bar{\rho}$ satisfies $\bar{\rho} \in \Sigma_{\bar{\rho}}$ where

$$\Sigma_{\bar{\rho}} := \{\bar{\rho} \,|\text{rank}\,(E(I_m - \bar{\rho})) = \text{rank}\,(E)\}\,. \tag{4}$$

Remark 1. It should be pointed out that outage faults are included in Assumption 2.1. For example, let

$$E = \begin{bmatrix} 1 & 1 \\ 0 & 0 \end{bmatrix}.$$

For the faulty case: the first actuator is healthy while the second one has an outage fault, i.e. $\bar{\rho} = \text{diag}\{0, 1\}$. The rank relation in Assumption 2.1 still holds. ∇

Under Assumption 2.1, a set Σ containing all tolerable fault modes can be defined by

$$\rho \in \Sigma := \left\{\rho = \text{diag}\{\rho_1, \cdots, \rho_m\} \,\middle|\, \underline{\rho}_i \leq \rho_i \leq \bar{\rho}_i,\ \bar{\rho} \in \Sigma_{\bar{\rho}}\right\}. \tag{5}$$

It should be pointed out that online information about ρ can be supplied by fault reconstruction schemes as described by Yan et al. (2007) or by fault estimation schemes such as Ye et al. (2006). Therefore, it is reasonable to suppose that there exists an estimate $\hat{\rho}$ for ρ. Furthermore, the adaptive estimation method used in Ye et al. (2006) can also guarantee $\underline{\rho}_i \leq \hat{\rho}_i \leq \bar{\rho}_i$. Thus, it is also reasonable to suppose that $\hat{\rho} \in \Sigma$.

Remark 2. It is worth pointing out that the estimation signal $\hat{\rho}$ is just for CA purposes, which is needed neither by the ISMO design nor in the stability analysis of the whole closed-loop FTC system. ∇

In actuator faulty scenario, in order to prevent faulty actuators from becoming more seriously damaged, the faulty actuators should be assigned with less control effort. The aim of a CA scheme is to redistributed the desired control efforts among all the physical actuators in faulty scenarios, which facilitates to assign less control efforts to faulty actuators and more control efforts to the healthy ones. To achieve

this aim, as proposed in Alwi et al. (2008), u is designed to minimize the following performance index

$$\min_u u^T \hat{W}^{-1} u \text{ subject to (3)} \tag{6}$$

where $\hat{W} = I_m - \hat{\rho}$. The optimal solution to (6) is

$$u = \hat{W} E^T (E \hat{W} E^T)^{-1} v := \hat{E}^\dagger v. \tag{7}$$

Objective. The objective of this paper is using the measurable output signal y to design an ISMO based sliding mode FTC law with the online CA scheme $u = \hat{E}^\dagger v$ for the LPV system (1)-(2) such that for any $\rho, \hat{\rho} \in \Sigma$, the unmeasurable states of the closed-loop system is asymptotically stable, and the measurable output y converges to zero in finite time.

3. Interval Sliding Mode Observer Formulation

In this paper, in order to transfer system (1)-(2) to a regular form, a similar assumption with Edwards et al. (1998) for the matrix pair $(C,\ B_0)$ is given as follows:

Assumption 3.1. The matrix pair $(C,\ B_0)$ satisfies $\text{rank}(CB_0) = \text{rank}(B_0) = p$.

From Assumption 3.1 and $B_0 = BE$, $p = \text{rank}(CB_0) = \text{rank}(CBE) \leq \text{rank}(CB) \leq \text{rank}(C) = p$. Therefore, $\text{rank}(CB) = \text{rank}(B) = p$. Then, based on the coordinate transformation used in Edwards et al. (2007), the triple (A, B, C) can be transformed into the following regular form

$$A = \begin{bmatrix} A_{11} & A_{12} \\ A_{21} & A_{22} \end{bmatrix},\ B = \begin{bmatrix} 0 \\ B_2 \end{bmatrix},\ C = \begin{bmatrix} 0 & I_p \end{bmatrix} \tag{8}$$

where $B_2 \in R^{p \times p}$ is a non-singular matrix. Thus, the system (1)-(2) can be written in the form

$$\dot{z}_s = A_{11} z_s + A_{12} z_2 + \Delta A_1(\theta(t)) \text{col}(z_s, z_2), \tag{9}$$

$$\dot{z}_2 = A_{21} z_s + A_{22} z_2 + \Delta A_2(\theta(t)) \text{col}(z_s, z_2) + B_2 v + B_2 v^f, \tag{10}$$

$$y = z_2 \tag{11}$$

for appropriate $\Delta A_1(\theta(t))$ and $\Delta A_2(\theta(t))$ where $v^f := -E\rho u$.

Since the triple $(A + \Delta A(\theta(t)), B, C)$ may be non-minimum phase, A_{11} in (9) may be an unstable matrix. To deal with this issue, a coordinate transformation $\text{col}(z_1, z_2) := T_o \text{col}(z_s, z_2)$ is introduced with

$$T_o = \begin{bmatrix} I_{n-p} & T \\ 0 & I_p \end{bmatrix} \tag{12}$$

where $T \in R^{(n-p) \times p}$ is a matrix which is specially introduced to address the non-minimum phase issue. It should be pointed out that in this paper there is no structural limitations on T as used in both Alwi et al. (2012) and Alwi et al. (2014), which

facilitates the relaxation of the minimum phase condition. In the new coordinates (z_1, z_2), system (9)-(11) becomes

$$\dot{z}_1 = A_1 z_1 + A_2 z_2 + [I_{n-p}, T]\Delta A(\theta(t)) T_o^{-1} z + TB_2 v + TB_2 v^f, \tag{13}$$

$$\dot{z}_2 = A_3 z_1 + A_4 z_2 + \Delta A_2(\theta(t)) T_o^{-1} z + B_2 v + B_2 v^f, \tag{14}$$

$$y = z_2 \tag{15}$$

where $z = \mathrm{col}(z_1, z_2)$, $A_1 = A_{11} + TA_{21}$, $A_2 = A_{12} + TA_{22} - (A_{11} + TA_{21})T$, $A_3 = A_{21}$, $A_4 = A_{22} - A_{21}T$ and $\Delta A(\theta(t)) = \mathrm{col}(\Delta A_1(\theta(t)), \Delta A_2(\theta(t)))$. Note that T should be designed such that A_1 is a Hurwitz matrix.

To formulate the ISMO, the interval bounds for $[I_{n-p}, T]\Delta A(\theta(t)) T_o^{-1} z$ and $TB_2 v^f$ appearing in (13)-(14) should be estimated. To do that, as in Efimov et al. (2016), Lamouchi et al. (2018) and Chebotarev et al. (2015), the following assumption for $\Delta A(\cdot)$ is needed:

Assumption 3.2. There are known matrices $\Delta A_1 > 0$ and $\Delta A_2 > 0$ such that

$$-\Delta A_1 \leq \Delta A_1(\theta(t)) \leq \Delta A_1,\ \Delta A_2 \leq \Delta A_2(\theta(t)) \leq \Delta A_2 \text{ for all } \theta(t) \in \Pi. \tag{16}$$

In addition, the following lemma is also needed and introduced as follows:

Lemma 3.3. *Let $x \in R^n$ be a vector such that $\underline{x} \leq x \leq \bar{x}$ for some $\underline{x}$, $\bar{x} \in R^n$. If $-\Delta A \leq A \leq \Delta A$ for some $\Delta A > 0$, then*

$$-\Delta A(\bar{x}^+ + \underline{x}^-) \leq Ax \leq \Delta A(\bar{x}^+ + \underline{x}^-). \tag{17}$$

Proof. The equation (17) follows straightforwardly from Lemma 2 in Efimov et al. (2012) by choosing $\bar{A}^+ = \Delta A$, $\bar{A}^- = 0$, $\underline{A}^+ = 0$ and $\underline{A}^- = \Delta A$. □

Let $\bar{z}_1$, $\bar{z}_2$, $\underline{z}_1$ and $\underline{z}_2$ represent estimates of the upper bounds and lower bounds for z_1 and z_2, respectively. Then, for the state $z = \mathrm{col}(z_1, z_2)$, an interval bound is chosen as $\underline{z} \leq z \leq \bar{z}$ where

$$\underline{z} = \mathrm{col}(\underline{z}_1, y),\ \bar{z} = \mathrm{col}(\bar{z}_1, y), \tag{18}$$

and thus, for $T_o^{-1} z$,

$$T_o^{-1}\underline{z} = \begin{bmatrix} \underline{z}_1 - Tz_2 \\ z_2 \end{bmatrix} \leq T_o^{-1} z = \begin{bmatrix} z_1 - Tz_2 \\ z_2 \end{bmatrix} \leq \begin{bmatrix} \bar{z}_1 - Tz_2 \\ z_2 \end{bmatrix} = T_o^{-1}\bar{z}. \tag{19}$$

Remark 3. In (18), a special structure is employed for $\underline{z}$ and $\bar{z}$ using y instead of $\underline{z}_2$ and $\bar{z}_2$. The advantage is that no extra restriction on T is needed to guarantee that (19) holds. ∇

Then, based on Lemma 3.3, for $\Delta A_1(\theta(t)) T_o^{-1} z$ and $T\Delta A_2(\theta(t)) T_o^{-1} z$, it follows from (16) and (19) that

$$\begin{aligned} -\Delta A_1 T_o^{-1}\left(\bar{z}^+ + \underline{z}^-\right) \leq & \Delta A_1(\theta(t)) T_o^{-1} z \leq \Delta A_1 T_o^{-1}\left(\bar{z}^+ + \underline{z}^-\right), \\ -|T|\Delta A_2 T_o^{-1}\left(\bar{z}^+ + \underline{z}^-\right) \leq & T\Delta A_2(\theta(t)) T_o^{-1} z \leq |T|\Delta A_2 T_o^{-1}\left(\bar{z}^+ + \underline{z}^-\right). \end{aligned}$$

Thus,

$$-[I_{n-p},|T|]\Delta A T_o^{-1}\left(\bar{z}^+ + \underline{z}^-\right) \leq [I_{n-p},T]\Delta A\left(\theta(t)\right)T_o^{-1}z \leq [I_{n-p},|T|]\Delta A T_o^{-1}\left(\bar{z}^+ + \underline{z}^-\right). \tag{20}$$

Let $\bar{v}_f$ and $\underline{v}_f$ represent estimates of the upper bound and lower bound for v_f respectively. For all $\rho \in \Sigma$, using results from Chebotarev et al. (2015), $-E^+ \leq -E\rho \leq E^-$. By defining

$$\underline{E}_i := \begin{cases} -E_i^+, & \text{if } u_i \geq 0, \\ E_i^-, & \text{if } u_i < 0, \end{cases} \quad \bar{E}_i := \begin{cases} E_i^-, & \text{if } u_i \geq 0, \\ -E_i^+, & \text{if } u_i < 0, \end{cases}$$

and denoting $\underline{E} = [\underline{E}_1, \cdots, \underline{E}_m]$ and $\bar{E} = [\bar{E}_1, \cdots, \bar{E}_m]$, it follows

$$\underline{E}u = \underline{v}^f \leq v^f \leq \bar{v}^f = \bar{E}u. \tag{21}$$

Since

$$TB_2 = (T^+ - T^-)(B_2^+ - B_2^-) = \Psi_1(T,B_2) - \Psi_2(T,B_2)$$

where

$$\Psi_1(\cdot) = (T^+B_2^+ + T^-B_2^-) = \begin{bmatrix} T^+ & T^- \end{bmatrix}\begin{bmatrix} B_2^+ \\ B_2^- \end{bmatrix},$$
$$\Psi_2(\cdot) = (T^+B_2^- + T^-B_2^+) = \begin{bmatrix} T^- & T^+ \end{bmatrix}\begin{bmatrix} B_2^+ \\ B_2^- \end{bmatrix},$$

and the positive property $\Psi_1(\cdot) \geq 0$ and $\Psi_2(\cdot) \geq 0$, it follows from Chebotarev et al. (2015) that

$$\Psi_1(\cdot)\underline{v}^f - \Psi_2(\cdot)\bar{v}^f \leq TB_2v^f \leq \Psi_1(\cdot)\bar{v}^f - \Psi_2(\cdot)\underline{v}^f. \tag{22}$$

Since the sliding mode techniques will be introduced for ISMO design, a useful fact associated with the sliding mode technique related to interval observers is summarized as follows:

Lemma 3.4. *Consider the following* 1*st order system*

$$\dot{x} = ax + d(t) - k\text{sign}(x), x(0) = x_0 > 0,\ d(t) \in R \tag{23}$$

where a is a negative scalar. If $k \geq |d| + \eta$ with η being any positive constant, then $x(t) \geq 0$ for $t \geq 0$, and $x(t) = 0$ after a finite time.

Proof. Since $k \geq |d| + \eta$, $x\dot{x} = ax^2 - \eta|x| \leq -\eta|x|$, which means that the *reachability condition* for sliding is satisfied. Once x reaches the sliding surface $\{x = 0\}$ it is forced to remain on it thereafter. Thus, $x(t) \geq 0$ for $t \geq 0$, and $x(t) = 0$ after a finite time. Therefore, it is concluded that the state in system (23) satisfies $x(t) \geq 0$ for $t \geq 0$ and $x(t) = 0$ after a finite time. □

Lemma 3.4 shows that for the 1st order system (23), the discontinuous sliding mode function with large enough gain is able to ensure that the ideal solution keeps positive, which implies that the sliding mode technique facilitates interval observer design in this regard. This result will be extended to nth systems in the following lemma.

Lemma 3.5. *Consider the nth order system*

$$\dot{x} = Ax + d(t) - k\text{sign}(x), x(0) > 0,\ d(t) \in R^n \tag{24}$$

where A is a negative definite diagonal matrix. If $k \geq \|d\| + \eta$ with η being any positive constant, then $x(t) \geq 0$ for $t \geq 0$, and $x(t) = 0$ after a finite time.

Proof. For any component x_i of x, $i = 1, \cdots, n$, based on Lemma 3.4, $x_i(t) \geq 0$ for $t \geq 0$ and $x_i(t) = 0$ after a finite time. Therefore, $x(t) = \text{col}(x_1(t), \cdots, x_n(t)) \geq 0$ for $t \geq 0$, and $x(t) = 0$ after a finite time. □

Therefore, using the interval bounds provided by (20) and (22) and the fact presented by Lemma 3.4, the structure of the ISMO for system (13)-(15) is proposed as

$$\dot{\bar{z}}_1 = A_1\bar{z}_1 + A_2y + [I, |T|]\Delta AT_0^{-1}\left(\bar{z}^+ + \underline{z}^-\right) + TB_2v + \Psi_1(\cdot)\bar{v}^f - \Psi_2(\cdot)\underline{v}^f, \tag{25}$$

$$\dot{\underline{z}}_1 = A_1\underline{z}_1 + A_2y - [I, |T|]\Delta AT_0^{-1}\left(\bar{z}^+ + \underline{z}^-\right) + TB_2v + \Psi_1(\cdot)\underline{v}^f - \Psi_2(\cdot)\bar{v}^f, \tag{26}$$

$$\dot{\bar{z}}_2 = A_3\bar{z}_1 + A_4\bar{z}_2 + B_2v + L(\bar{z}_2 - z_2) - \bar{K}\nu, \tag{27}$$

$$\dot{\underline{z}}_2 = A_3\underline{z}_1 + A_4\bar{z}_2 + B_2v - L(z_2 - \underline{z}_2) + \underline{K}\nu \tag{28}$$

where the initial values satisfy $\underline{z}_1(0) \leq z_1(0) \leq \bar{z}_1(0)$ and $\underline{z}_2(0) \leq z_2(0) \leq \bar{z}_2(0)$, and the matrices L, $\bar{K}$ and $\underline{K}$ are to be determined later. The nonlinear function ν is designed as $\nu = \text{col}(\text{sign}(\bar{z}_2 - z_2), \text{sign}(z_2 - \underline{z}_2))$.

Remark 4. It is worth pointing out that the structure design of the ISMO in (25)-(28) is based on the standard regular form of sliding mode observer as the Utkin-observer. However, it is very different from the Utkin-observer because the designed ISMO is able to generate interval estimates for z_1 and z_2, i.e. $\underline{z}_1 \leq z_1 \leq \bar{z}_1$ and $\underline{z}_2 \leq z_2 \leq \bar{z}_2$.∇

Remark 5. The proposed ISMO (25)-(28) can generate tighter interval estimates than other interval observers which do not use sliding mode techniques such as the ones in Chebotarev et al. (2015) and Mazenc et al. (2011). This is because if the gain matrices $\bar{K}$ and $\underline{K}$ are chosen properly, then from Lemma 3.5, $\underline{z}_2 = z_2 = \bar{z}_2$ holds in finite time when a sliding motion occurs, which is tighter than $\underline{z}_2 \leq z_2 \leq \bar{z}_2$ obtained using other interval observers. ∇

Define a set of errors as follows:

$$\begin{array}{lll} \bar{e}_1 := \bar{z}_1 - z_1, & \underline{e}_1 := z_1 - \underline{z}_1, & e_1 := \text{col}(\bar{e}_1, \underline{e}_1), \\ \bar{e}_2 := \bar{z}_2 - z_2, & \underline{e}_2 := z_2 - \underline{z}_2, & e_2 := \text{col}(\bar{e}_2, \underline{e}_2). \end{array}$$

By comparing observer (25)-(28) with system (13)-(14), the error system can be expressed in a compact form as

$$\dot{e}_1 = A_{1o}e_1 + \Phi_o(e_1, z) + \Psi_o(u), \tag{29}$$

$$\dot{e}_2 = A_{3o}e_1 + A_{4o}e_2 + \Phi_{2o}(z) + B_{2o}E\rho u - K_o\nu \tag{30}$$

where

$$A_{1o} = \left[\begin{array}{c|c} A_1 & 0 \\ \hline 0 & A_1 \end{array}\right], A_{3o} = \left[\begin{array}{c|c} A_3 & 0 \\ \hline 0 & A_3 \end{array}\right],$$
$$A_{4o} = \left[\begin{array}{c|c} A_4+L & 0 \\ \hline 0 & A_4+L \end{array}\right], B_{2o} = \left[\begin{array}{c} B_2 \\ -B_2 \end{array}\right],\ K_o = \left[\begin{array}{c} \bar{K} \\ \underline{K} \end{array}\right],$$
$$\Psi_o(\cdot) = \left[\begin{array}{c} \Psi_1(\cdot)\bar{v}^f - \Psi_2(\cdot)\underline{v}^f - TB_2v^f \\ TB_2v^f - \Psi_1(\cdot)\underline{v}^f + \Psi_2(\cdot)\bar{v}^f \end{array}\right],$$
$$\Phi_o(\cdot) = \left[\begin{array}{c} [I_{n-p}, |T|]\Delta A|T_o|\left(\bar{z}^+ + \underline{z}^-\right) - [I_{n-p}, T]\Delta A(\theta(t))T_o^{-1}z \\ [I_{n-p}, T]\Delta A(\theta(t))T_o^{-1}z + [I_{n-p}, |T|]\Delta A|T_o|\left(\bar{z}^+ + \underline{z}^-\right) \end{array}\right],$$
$$\Phi_{2o}(\cdot) = \left[\begin{array}{c} -\Delta A_2(\theta(t)) \\ \Delta A_2(\theta(t)) \end{array}\right] T_o^{-1}z.$$

For this error system in (29)-(30), consider the sliding function $s_o = e_2$ and the sliding surface

$$\mathcal{S}_o = \{(e_1, e_2)|s_o = 0\}. \tag{31}$$

Then, the following proposition is ready to be presented.

Proposition 3.6. *Under Assumptions 2.1-3.2, the solution for system (25)-(28) satisfies*

$$\underline{z}_1 \le z_1 \le \bar{z}_1,\ \underline{z}_2 \le z_2 \le \bar{z}_2,\quad \forall\ t \ge 0, \tag{32}$$

if there exist matrices T, L, $\bar{K}$ and $\underline{K}$ such that

(1) A_{1o} is the Metzler matrix,
(2) $L = -A_4 + \bar{A}_4$ where $\bar{A}_4$ is a negative diagonal matrix,
(3) $K_o = k_o(\bar{z}_1, \underline{z}_1, y, u)I_{2p}$ where

$$\begin{aligned} k_o(\cdot) \ge & 2\|A_{3o}\|(\|\bar{z}_1\| + \|\underline{z}_1\|) + 2\|\Delta A_2\|\|T_o^{-1}\|(\|\bar{z}_1\| + \|\underline{z}_1\| + \|y\|) \\ & + m\|B_{2o}E\|\|u\| + \eta_o \end{aligned}$$

where η_o is any positive scalar.

Furthermore, the sliding function s_o is driven to the sliding surface $\mathcal{S}_o$ in finite time and remains on it thereafter.

Proof. It can be seen from (20) that the right hand side in (20) minus the middle term leads to the first row of Φ_o. The second row of Φ_o results from the middle term in (20) minus the left hand side term. In addition, the precondition of (20) is that $\underline{z}_1 \le z_1 \le \bar{z}_1$. Thus, it follows that if $\underline{z}_1 \le z_1 \le \bar{z}_1$, then $\Phi_o(\cdot) \ge 0$. With an initial condition satisfying $\underline{z}_1(0) \le z_1(0) \le \bar{z}_1(0)$, it follows that $e_1(0) \ge 0$. Since A_{1o} is a Metzler matrix, and from (22) $\Psi_o(\cdot) > 0$, based on the positive system theory results in Farina et al. (2011), $e_1(t) \ge 0$ for $t \ge 0$. Therefore, the relation $\underline{z}_1 \le z_1 \le \bar{z}_1$ holds.

In the sequel, the bounds for items $A_{3o}e_1 + \Phi_{2o}(z)$ and $B_{2o}E\rho u$ are estimated. Due to the fact that for any vector $x \in R^n$ satisfying $\underline{x} \le x \le \bar{x}$ with $\underline{x},\ \bar{x} \in R^n$,

$\|x\| \leq \|\bar{x}\| + \|\underline{x}\|$, $\|e_1\| \leq \|\bar{z}_1 - z_1\| + \|z_1 - \underline{z}_1\| \leq 2(\|\bar{z}_1\| + \|\underline{z}_1\|)$, and

$$\|A_{3o}e_1 + \Phi_{2o}(z)\| \leq 2\|A_{3o}\|(\|\bar{z}_1\| + \|\underline{z}_1\|) + 2\|\Delta A_2\|\|T_o^{-1}\|\|(\|\bar{z}_1\| + \|\underline{z}_1\| + \|y\|) \tag{33}$$

where the relation $\|\Delta A_2(\theta(t))\| \leq \|\Delta A_2\|$ is used to obtain above inequality. Also, since $0 \leq \rho \leq I_m$, $\|\rho\| \leq 1$, $\|B_{2o}E\rho u\| \leq \|B_{2o}E\|\|u\|$. Thus, $k_o(\cdot)$ in the Proposition 3.6 satisfies that $k_o(\cdot) \geq \|A_{3o}e_1 + \Phi_{2o}(z) + B_{2o}E\rho u\|$. Since $\bar{A}_{22}$ is a negative diagonal matrix, all conditions in Lemma 3.5 are satisfied. Therefore, $e_2 \geq 0$ for $t \geq 0$ and further, s_o is driven to the sliding surface $\mathcal{S}_o$ in finite time and remains on it thereafter.

Hence, the result follows. □

Remark 6. It should be pointed out that Proposition 3.6 just presents the conditions to guarantee interval estimates of (32). The stability analysis will be presented in the following section. In addition, in order to ensure A_{1o} in (29) to be Metzler, the matrix $A_1 = A_{11} + TA_{21}$ should be Metzler, which can be achieved by selecting a suitable design parameter T given in (12). The details will be shown in the following section.∇

4. Sliding Mode Control Law Design

The observer (25)-(28) possesses two special characteristics: one is that if both $\bar{z}_1$ and $\underline{z}_1$ converge to zero asymptotically, then z_1 converges to zero asymptotically as well; the other is that during sliding on $\mathcal{S}_o$, if $0.5(\bar{z}_2 + \underline{z}_2)$ (the interval average) is driven to zero in finite time, then z_2 is also driven to zero in finite time. So if v in (25)-(28) forces both $\bar{z}_1$ and $\underline{z}_1$ to converge to zero asymptotically and $0.5(\bar{z}_2 + \underline{z}_2)$ to zero in finite time, then the control objective is achieved. Therefore, in this section, the sliding mode control law will be built around the observer (25)-(28).

In the coordinates ζ_1 and ζ_2 where $\zeta_1 = \text{col}(\bar{z}_1, \underline{z}_1) \in R^{2(n-p)}$ and $\zeta_2 = 0.5(\bar{z}_2 + \underline{z}_2) \in R^p$, it follows from (25)-(28) that

$$\dot{\zeta}_1 = A_{1c}\zeta_1 + N_1 y + T_G G(\bar{z}_1, \underline{z}_1, y) + T_B B_{1c} v + T_{\Delta 1}\Delta B_{1c}\bar{E}\hat{E}^\dagger v + T_{\Delta 2}\Delta B_{1c}\underline{E}\hat{E}^\dagger v, \tag{34}$$

$$\dot{\zeta}_2 = A_{3c}\zeta_1 + A_{4c}\zeta_2 + N_2 y + B_2 v + K_c \nu \tag{35}$$

where

$$A_{1c} = \left[\begin{array}{c|c} A_1 & 0 \\ \hline 0 & A_1 \end{array}\right], \quad G(\cdot) = \Delta A T_o^{-1}(\bar{z}^+ + \underline{z}^-),$$
$$N_1 = \left[\begin{array}{c} A_2 \\ A_2 \end{array}\right], \quad B_{1c} = B_2,$$
$$\Delta B_{1c} = \left[\begin{array}{c} B_2^+ \\ B_2^- \end{array}\right], \quad A_{3c} = 0.5A_3[I_{n-p}, I_{n-p}],$$
$$N_2 = -L, \quad A_{4c} = A_2 + L, \; K_c = 0.5(\underline{K} - \bar{K}).$$

In addition, by using the fact that $T = T^+ - T^-$ and $|T| = T^+ - T^-$,

$$
\begin{aligned}
T_G &= \left[\begin{array}{cc} I_{n-p} & |T| \\ -I_{n-p} & -|T| \end{array} \right] = \left[\begin{array}{cc} I_{n-p} & T^+ + T^- \\ -I_{n-p} & -T^+ - T^- \end{array} \right], \\
T_B &= \left[\begin{array}{c} T \\ T \end{array} \right] = \left[\begin{array}{c} T^+ - T^- \\ T^+ - T^- \end{array} \right], \\
T_{\Delta 1} &= \left[\begin{array}{cc} T^+ & T^- \\ -T^- & -T^+ \end{array} \right],\ T_{\Delta 2} = \left[\begin{array}{cc} -T^- & -T^+ \\ T^+ & T^- \end{array} \right].
\end{aligned}
$$

The corresponding relationships among T_G, T_B, $T_{\Delta 1}$ and $T_{\Delta 2}$ are given as follows

$$
\begin{aligned}
T_G &= \left[\begin{array}{c|c} I_{n-p} & T_{\Delta 1} \left[\begin{array}{c} I_{n-p} \\ I_{n-p} \end{array} \right] \\ I_{n-p} & \end{array} \right] = \left[\begin{array}{cc} I_{n-p} & 0 \\ I_{n-p} & 0 \end{array} \right] + T_{\Delta 1} \left[\begin{array}{cc} 0 & I_{n-p} \\ 0 & I_{n-p} \end{array} \right], \\
T_B &= T_{\Delta 1} \left[\begin{array}{c} I_{n-p} \\ -I_{n-p} \end{array} \right],\ T_{\Delta 2} = T_{\Delta 1} \left[\begin{array}{cc} 0 & -I_{n-p} \\ -I_{n-p} & 0 \end{array} \right].
\end{aligned} \tag{36}
$$

For system (34)-(35), consider the sliding function $s_c = \zeta_2$ and sliding surface

$$\mathcal{S}_c = \{(\zeta_1, \zeta_2) | s_c = 0\}.$$

For the closed-loop system (29)-(30) and (34)-(35), consider the sliding surface

$$\mathcal{S}_u = \mathcal{S}_o \cap \mathcal{S}_c = \{(e_1, e_2, \zeta_1, \zeta_2) | s_o = 0,\ s_c = 0\}. \tag{37}$$

4.1. Stability analysis for the sliding motion

The sliding motion associated with $\mathcal{S}_u$ is determined by e_1 in (29) and ζ_1 in (34). Since the stabilities of e_1 and ζ_1 are synchronous, the sliding motion can be determined only by the reduced order system (34). If a control law can be designed to introduce a sliding mode associated with the sliding surface $\mathcal{S}_u$, then during sliding, $\dot{s}_c = s_c = 0$ and $\dot{s}_o = s_o = 0$. Thus, it follows from (30) and (35) that

$$A_{3o} e_1 + \Phi_{2o}(z) + B_{2o} E \rho u - K_o \nu = 0, \tag{38}$$

$$A_{3c} \zeta_1 + B_2 v + K_c \nu = 0,\ y = \zeta_2 = 0. \tag{39}$$

In the sequel, under equations (38) and (39), items $G(\bar{z}_1, \underline{z}_1, y)$, $B_{1c} v$, $\Delta B_{1c} \bar{E} \hat{E}^\dagger v$ and $\Delta B_{1c} \underline{E} \hat{E}^\dagger v$ in (34) will be specified by functions of z_1.

From (12) and (18),

$$
\begin{aligned}
T_0^{-1} \bar{z}^+ &= \left[\begin{array}{cc} I & -T \\ 0 & I \end{array} \right] \left[\begin{array}{c} \bar{z}_1^+ \\ y^+ \end{array} \right] = \left[\begin{array}{cc} I_{n-p} & 0 \\ 0 & 0 \end{array} \right] \zeta_1^+ := \bar{S} \zeta_1^+, \\
T_0^{-1} \underline{z}^- &= \left[\begin{array}{cc} I & -T \\ 0 & I \end{array} \right] \left[\begin{array}{c} \underline{z}_1^- \\ y^- \end{array} \right] = \left[\begin{array}{cc} 0 & I_{n-p} \\ 0 & 0 \end{array} \right] \zeta_1^- := \underline{S} \zeta_1^-, \\
T_0^{-1} z &= \left[\begin{array}{cc} I & -T \\ 0 & I \end{array} \right] \left[\begin{array}{c} z_1 \\ y \end{array} \right] = \left[\begin{array}{c} I_{n-p} \\ 0 \end{array} \right] z_1 := M z_1,
\end{aligned}
$$

and thus, it follows from $\zeta_1^+ = \frac{1}{2}(\zeta_1 + |\zeta_1|)$ and $\zeta_1^- = \frac{1}{2}(-\zeta_1 + |\zeta_1|)$ that

$$G(\bar{z}_1, \underline{z}_1, y) = \Delta A(\bar{S} - \underline{S})\zeta_1 + \Delta A(\bar{S} + \underline{S})|\zeta_1| := \Delta A_{1c}\zeta_1 + \Delta \bar{A}_{1c}|\zeta_1| \tag{40}$$

where $\Delta A_{1c} = \Delta A(\bar{S} - \underline{S})$ and $\Delta \bar{A}_{1c} = \Delta A(\bar{S} + \underline{S})$.

It is worth pointing that there exists a $T_{co} = 0.5[-I_p, I_p]$ such that

$$K_c = T_{co}K_o,\ T_{co}A_{3o} = 0.5A_3[-I_{n-p}, I_{n-p}], \tag{41}$$

$$T_{co}\Phi_{2o}(z) = \Delta A_2(\theta(t))T_o^{-1}z = \Delta A_2(\theta(t))Mz_1,\ T_{co}B_{2o} = -B_2. \tag{42}$$

Then, it follows from (38), (39) and $u = \hat{E}^\dagger v$ that $B_2 v = -A_{3c}\zeta_1 - K_c\nu = -A_{3c}\zeta_1 - T_{co}(A_{3o}e_1 + \Phi_{2o}(z) + B_{2o}E\rho\hat{E}^\dagger v)$, which implies

$$\hat{B}_2 v := B_2(I_p - E\rho\hat{E}^\dagger)v = -A_{3c}\zeta_1 - T_{co}(A_{3o}e_1 + \Phi_{2o}(z)) = -(A_3 + \Delta A_2(\theta(t))M)z_1$$

where $\hat{B}_2 = B_2(I_p - E\rho\hat{E}^\dagger) = B_2E(I_m - \rho)\hat{W}E^T(E\hat{W}E^T)^{-1}$. The matrix $\hat{B}_2$ is revertible because for all $\rho, \hat{\rho} \in \Sigma$, $E(I_m - \rho)\hat{W}E^T$ is revertible. Thus,

$$v = -\hat{B}_2^{-1}(A_3 + \Delta A_2(\theta(t))M)z_1 \tag{43}$$

and $B_{1c}v$, $\Delta B_{1c}\bar{E}\hat{E}^\dagger v$ and $\Delta B_{1c}\underline{E}\hat{E}^\dagger v$ follow.

Therefore, it follows from (40) and (43) that the dynamic of ζ_1 on sliding surface $\mathcal{S}_u$ is obtained by

$$\begin{aligned}\dot{\zeta}_1 =& A_{1c}\zeta_1 + T_G\Delta A_{1c}\zeta_1 + T_G\Delta\bar{A}_{1c}|\zeta_1| - T_B B_2\hat{B}_2^{-1}(A_3 + \Delta A_2(\theta(t))M)z_1 \\ & - T_{\Delta 1}\Delta B_{1c}\bar{E}\hat{E}^\dagger\hat{B}_2^{-1}(A_3 + \Delta A_2(\theta(t))M)z_1 \\ & - T_{\Delta 2}\Delta B_{1c}\underline{E}\hat{E}^\dagger\hat{B}_2^{-1}(A_3 + \Delta A_2(\theta(t))M)z_1.\end{aligned} \tag{44}$$

The stability of (44) will be presented in the following. It should be pointed out that it has been proven in Hao et al. (2013) that for any $\hat{\rho} \in \Sigma$, there exists a positive scalar α such that

$$E\hat{W}E^T \succcurlyeq \alpha I_p. \tag{45}$$

Thus, $\hat{E}^\dagger$ is uniformly bounded with respect to $\hat{\rho} \in \Sigma$, that is

$$\|\hat{E}^\dagger\| = \|\hat{W}E^T(E\hat{W}E^T)^{-1}\| \le \|\hat{W}E^T\|\|(E\hat{W}E^T)^{-1}\| \le \alpha\|E\| := \gamma_0 \tag{46}$$

where γ_0 is a constant independent of $\hat{\rho}$. In addition, suppose that

$$\min_{\rho\in\Sigma}\|I_m - \rho\| = \gamma_\rho \tag{47}$$

where γ_ρ is a known positive scalar. Then, $\|\hat{B}_2^{-1}\| \le \|B_2^{-1}\|\|(E(I_m - \rho)\hat{E}^\dagger)^{-1}\| \le \frac{\|B_2^{-1}\|}{\gamma_\rho}$. By denoting $\|\Delta B_{1c}E\| := \gamma_1$, $\|\Delta\bar{A}_{1c}\| := \gamma_2$, $\|B_2^{-1}\| := \gamma_3$, $\|A_3\| :=$

γ_4, $\|A_2(\theta(t))M\| := \gamma_5$, and recalling (46), it follows that

$$\|B_2\hat{B}_2^{-1}A_3\| \leq \frac{\|B_2\|\gamma_3\gamma_4}{\gamma_\rho},\ \|B_2\hat{B}_2^{-1}\Delta A_2(\theta(t))M\| \leq \frac{\|B_2\|\gamma_3\gamma_5}{\gamma_\rho}, \tag{48}$$

$$\|\Delta B_{1c}\bar{E}\hat{E}^\dagger\hat{B}_2^{-1}A_3\| \leq \frac{\gamma_0\gamma_1\gamma_3\gamma_4}{\gamma_\rho},\ \|\Delta B_{1c}\bar{E}\hat{E}^\dagger\hat{B}_2^{-1}\Delta A_2(\theta(t))M\| \leq \frac{\gamma_0\gamma_1\gamma_3\gamma_5}{\gamma_\rho}, \tag{49}$$

$$\|\Delta B_{1c}\underline{E}\hat{E}^\dagger\hat{B}_2^{-1}A_3\| \leq \frac{\gamma_0\gamma_2\gamma_3\gamma_4}{\gamma_\rho},\ \|\Delta B_{1c}\underline{E}\hat{E}^\dagger\hat{B}_2^{-1}\Delta A_2(\theta(t))M\| \leq \frac{\gamma_0\gamma_2\gamma_3\gamma_5}{\gamma_\rho}. \tag{50}$$

Then, the following proposition is ready to be presented.

Proposition 4.1. *The sliding motion (44) is asymptotically stable if there exist matrices T, $P = P^T \succ 0$ and $Q = Q^T \succ 0$ such that for given positive scalars ϵ_i, $i = 1, 2, 3, 4$,*

$$\begin{aligned} A_c^TP + PA_c &+ \epsilon_1 PT_BT_B^TP + \epsilon_2 PT_GT_G^TP \\ &+ \epsilon_3 PT_{\Delta 1}T_{\Delta 1}^TP + \epsilon_4 PT_{\Delta 2}T_{\Delta 2}^TP + \gamma I_{2(n-p)} \prec -Q,\ \forall\ \rho, \hat{\rho} \in \Sigma \end{aligned} \tag{51}$$

where

$$\gamma = \epsilon_1^{-1}\gamma_3^2 + \epsilon_2^{-1}\|B_2\|^2\left(\frac{\gamma_3(\gamma_4+\gamma_5)}{\gamma_\rho}\right)^2 + \epsilon_3^{-1}\left(\frac{\gamma_0\gamma_1\gamma_3(\gamma_4+\gamma_5)}{\gamma_\rho}\right)^2 + \epsilon_4^{-1}\left(\frac{\gamma_0\gamma_2\gamma_3(\gamma_4+\gamma_5)}{\gamma_\rho}\right)^2$$

and $A_c = A_{1c} + T_G\Delta A_{1c}$.

Proof. Choose $V_c = \zeta_1^TP\zeta_1$ as a Lyapunov function candidate. Then, the time derivative of V_c along (44) is obtained by

$$\begin{aligned} \dot{V}_c =& \zeta_1^T\left(A_c^TP + PA_c\right)\zeta_1 - 2\zeta_1^TPT_G\Delta\bar{A}_{1c}|\zeta_1| - 2\zeta_1^TPT_BB_2\hat{B}_2^{-1}(A_3 + \Delta A_2(\theta(t))M)z_1 \\ &- 2\zeta_1^TPT_{\Delta 1}\Delta B_{1c}\bar{E}\hat{E}^\dagger(A_3 + \Delta A_2(\theta(t))M)z_1 \\ &- 2\zeta_1^TPT_{\Delta 2}\Delta B_{1c}\underline{E}\hat{E}^\dagger(A_3 + \Delta A_2(\theta(t))M)z_1 \\ \leq& \zeta_1^T\left(A_c^TP + PA_c\right)\zeta_1 + \epsilon_1\zeta_1^TPT_GT_G^TP\zeta_1 + \epsilon_1^{-1}\gamma_3^2\|\zeta_1\|^2 \\ &+ \epsilon_2\zeta_1^TPT_BT_B^TP\zeta_1 + \epsilon_2^{-1}\|B_2\|^2\left(\frac{\gamma_3(\gamma_4+\gamma_5)}{\gamma_\rho}\right)^2\|\zeta_1\|^2 \\ &+ \epsilon_3\zeta_1^TPT_{\Delta 1}T_{\Delta 1}^TP\zeta_1 + \epsilon_3^{-1}\left(\frac{\gamma_0\gamma_1\gamma_3(\gamma_4+\gamma_5)}{\gamma_\rho}\right)^2\|\zeta_1\|^2 \\ &+ \epsilon_4\zeta_1^TPT_{\Delta 2}T_{\Delta 2}^TP\zeta_1 + \epsilon_4^{-1}\left(\frac{\gamma_0\gamma_2\gamma_4(\gamma_4+\gamma_5)}{\gamma_\rho}\right)^2\|\zeta_1\|^2 \\ \leq& -\zeta_1^T\left(A_c^TP + PA_c + \epsilon_1PT_GT_G^TP + \epsilon_2PT_BT_B^TP + \epsilon_3PT_{\Delta 1}T_{\Delta 1}^TP + \epsilon_4PT_{\Delta 2}T_{\Delta 2}^TP\right)\zeta_1 \\ &+ \gamma\|\zeta_1\|^2 \leq -\zeta_1Q\zeta_1^T \end{aligned}$$

where the second inequality is obtained based on the well-known inequality $2X^TY \leq \epsilon X^TX + \epsilon^{-1}Y^TY$ for any scalar $\epsilon > 0$, and the fact that $\|z_1\|^2 \leq \|\zeta_1\|^2$. Therefore, ζ_1 is asymptotically stable.

Hence, the result follows. □

Remark 7. Using Schur lemma, (51) is equivalent to the following matrix inequality with respect to $P = P^T \succ 0$, $Q = Q^T \succ 0$, T_G, T_B, $T_{\Delta 1}$ and $T_{\Delta 2}$

$$\begin{bmatrix} A_c^T P + P A_c & PT_B & PT_G & PT_{\Delta 1} & PT_{\Delta 2} & I_{2(n-p)} \\ * & -\frac{\epsilon_1^{-1}}{2} I_n & 0 & 0 & 0 & 0 \\ * & * & -\frac{\epsilon_2^{-1}}{2} I_n & 0 & 0 & 0 \\ * & * & * & -\frac{\epsilon_3^{-1}}{2} I_{2p} & 0 & 0 \\ * & * & * & * & -\frac{\epsilon_4^{-1}}{2} I_{2p} & 0 \\ * & * & * & * & * & -\gamma^{-1} I_{2(n-p)} + Q \end{bmatrix} \prec 0.$$

Then, under additional limitation $P = \mathrm{diag}\{P_1, P_1\}$ with $P_1 = P_1^T \succ 0$, based on the relation (36), the feasible solution issue in Proposition 4.1 can be converted to solving the following linear matrix inequalities (LMI) with respect to P_1, Y^+, Y^- and Q for given ϵ_i, $i = 1, 2, 3, 4$,

$$P_1 \succ 0, Q \succ 0, Y^+ \geq 0, Y^- \geq 0,$$

$$\begin{bmatrix} \Theta_A & \Theta_B & \Theta_G & \Theta_{\Delta_1} & \Theta_{\Delta_2} & I_{2(n-p)} \\ * & -\frac{\epsilon_1^{-1}}{2} I_n & 0 & 0 & 0 & 0 \\ * & * & -\frac{\epsilon_2^{-1}}{2} I_n & 0 & 0 & 0 \\ * & * & * & -\frac{\epsilon_3^{-1}}{2} I_{2p} & 0 & 0 \\ * & * & * & * & -\frac{\epsilon_4^{-1}}{2} I_{2p} & 0 \\ * & * & * & * & * & -\gamma^{-1} I_{2(n-p)} + Q \end{bmatrix} \prec 0$$

where $\Theta_A = A_{1c}^T P + P A_{1c} + \Theta_G \Delta A_{1c} + \Delta A_{1c}^T \Theta_G^T$,

$$\begin{aligned} \Theta_G =& P \begin{bmatrix} I_{n-p} & 0 \\ I_{n-p} & 0 \end{bmatrix} + \Theta_{\Delta 1} \begin{bmatrix} 0 & I_{n-p} \\ 0 & I_{n-p} \end{bmatrix}, \ \Theta_B = \Theta_{\Delta 1} \begin{bmatrix} I_{n-p} \\ -I_{n-p} \end{bmatrix}, \\ \Theta_{\Delta 1} =& \begin{bmatrix} Y^+ & 0 \\ 0 & -Y^+ \end{bmatrix} + \begin{bmatrix} 0 & Y^- \\ -Y^- & 0 \end{bmatrix}, \ \Theta_{\Delta 2} = \Theta_{\Delta 1} \begin{bmatrix} 0 & -I_{n-p} \\ -I_{n-p} & 0 \end{bmatrix}. \end{aligned}$$

Then, $T^+ = P_1^{-1} Y^+$ and $T^- = P_1^{-1} Y^-$. ∇

4.2. Reachability analysis

According to the sliding surface $\mathcal{S}_u$ in (37), the reachability of the whole closed-loop system consists of two parts: the reachability of the observer (25)-(28) associated with $\mathcal{S}_o$ and the reachability of control associated with $\mathcal{S}_c$. Proposition 3.6 has provided the reachability condition to guarantee the sliding modes associated with $\mathcal{S}_o$. From (38), during the sliding,

$$K_c \nu = T_{co} K_o \nu = T_{co} \left(A_{3o} e_1 + \Phi_{2o}(z) \right) - B_2 E \rho u.$$

Thus, it follows from (35) and the selection of sliding function $s_c = \zeta_2$ that

$$\begin{aligned}\dot{s}_c =& A_{3c}\zeta_1 + A_{4c}s_c + N_2 y + B_2 v + T_{co}\left(A_{3o}e_1 + \Phi_{2o}\left(z\right)\right) - B_2 E\rho u \\ =& A_{3c}\zeta_1 + A_{4c}s_c + N_2 y + T_{co}\left(A_{3o}e_1 + \Phi_{2o}\left(z\right)\right) + B_2 E(I_m - \rho)\hat{E}^{\dagger} v. \end{aligned} \tag{52}$$

where the control law v is designed by referring to the unit vector approach in Edwards et al. (1998) and is comprised of two components: a linear component v_l to stabilize the nominal linear system and a discontinuous component v_n. Specifically,

$$v = B_2^{-1}(v_l + v_n) \tag{53}$$

where

$$v_l = - A_{3c}\zeta_1 - A_{4c}s_c - N_2 y, \tag{54}$$

$$v_n = - k_c(t, \bar{z}_1, \underline{z}_1, y)\frac{s_c}{\|s_c\|}, \quad \text{if} \quad s_c \neq 0 \tag{55}$$

where $k_c(\cdot)$ satisfies

$$k_c(\cdot) \geq \frac{\|v_l\| + 2\|T_{co}\|(\|A_{3o}\|(\|\bar{z}_1\| + \|\underline{z}_1\|) + \|\Delta A_2\|\|T_o^{-1}\|\|(\|\bar{z}_1\| + \|\underline{z}_1\| + \|y\|)) + \eta_c}{\alpha}$$

with α being given by (45) and η_c being any positive scalar. Substituting (53) and (54) into (52) yields

$$\dot{s}_c = T_{co}\left(A_{3o}e_1 + \Phi_{2o}\left(z\right)\right) + B_2(E(I_m - \rho)\hat{E}^{\dagger})B_2^{-1}v_n - B_2 E\rho\hat{E}^{\dagger}B_2^{-1}v_l. \tag{56}$$

Then, based on (33), (54) and (55),

$$\begin{aligned} s_c^T\dot{s}_c =& s_c^T B_2(E(I_m - \rho)\hat{E}^{\dagger})B_2^{-1}v_n - s_c^T B_2 E\rho\hat{E}^{\dagger}B_2^{-1}v_l + s_c^T T_{co}\left(A_{3o}e_1 + \Phi_{2o}\left(z\right)\right) \\ \leq& \|s_c\|(-\alpha k_c(\cdot) + \|v_l\| + \|T_{co}\|\|A_{3o}e_1 + \Phi_{2o}\left(z\right)\|) \leq -\eta_c\|s_c\| \end{aligned}$$

where the second inequality is obtained from $B_2(E(I_m - \rho)\hat{E}^{\dagger})B_2^{-1} \geq \alpha I_p$ induced from (45) and $\|B_2 E\rho\hat{E}^{\dagger}B_2^{-1}\| \leq 1$. Thus, based on the reachability condition in Edwards et al. (1998), s_c is driven to the sliding surface $\mathcal{S}_c$ in finite time and remains on it thereafter.

Remark 8. The control law v given in (53) is based on but different from the well-known unit vector strategy in Edwards et al. (1998) in that v_l and v_n in (53) are built on the interval estimates generated by the designed ISMO such as ζ_1 in (54) and $\bar{z}_1, \underline{z}_1$ in (55). In addition, it should be noted that the discontinuous control law v_n in (55) may further damage the faulty actuator and makes the faulty scenario more serious. Therefore, it is necessary to replace v_n by $v_n = -k_c(t, \bar{z}_1, \underline{z}_1, y)\frac{s_c}{\|s_c\|+\delta}$ where δ is a positive constant based on practical control accuracy requirements. ∇

Therefore, recalling Propositions 3.6 and 4.1, the following theorem summarizes the developments in the proceeding section.

Theorem 4.2. *If the conditions in Propositions 3.6 and 4.1 are satisfied and v is designed as (53) with v_l and v_n being determined by (54) and (55) respectively, then*

z_1 converges to zero asymptotically, and z_2 converges to zero in finite time for all faults $\rho, \hat{\rho} \in \Sigma$.

Proof. Under the conditions of Proposition 3.6, if both $\bar{z}_1$ and $\underline{z}_1$ converge to zero asymptotically, then z_1 also converge to zero asymptotically. Also, during the sliding motion associated with $\mathcal{S}_o$, if ζ_2 converges to zero in finite time, then z_2 also converges to zero in finite time. Therefore, if all the conditions in Propositions 3.6 and 4.1 are satisfied, then z_1 converges to zero asymptotically, and z_2 converge to zero in finite time. □

Remark 9. It is more practical to consider system (1)-(2) with input and output uncertainties. In this case, the key issue to design an ISMO is to guarantee (19), (20) and (22) hold under sensor disturbances. Suppose that the output in (15) is expressed by $y = z_2 + \xi$ where ξ represents disturbances in the sensor measurements, and there is a known constant Ξ such that $|\xi(t)| \leq \Xi E_p$, i.e. $-\Xi E_p \leq \xi(t) \leq \Xi E_p$. For $z = \mathrm{col}(z_1, z_2)$, in order to guarantee $\underline{z} \leq z \leq \bar{z}$, $\underline{z}$ and $\bar{z}$ are chosen as $\underline{z} = \mathrm{col}(\underline{z}_1, y - \Xi E_p)$ and $\bar{z} = \mathrm{col}(\bar{z}_1, y + \Xi E_p)$ respectively, which are different from (18). Under this selection, in order to guarantee (19) holds, an extra condition $T \leq 0$ must be satisfied where T has been defined in (12). Then, both (20) and (22) also hold, and further, the ISMO developed in this paper can be extended easily to the case when the input and output have uncertainties using the approaches propagating uncertainties in Chebotarev et al. (2015), Efimov et al. (2016) and Lamouchi et al. (2018). Moreover, the control laws are still designed as (53), (54) and (55), but the gain in (55) should be redesigned to guarantee the reachability condition taking into account disturbances. However, it should be pointed out that on the sliding surface $s_c = 0$, $y = z_2 + \xi = 0$, i.e. $z_2 = -\xi$. Therefore, with input and output uncertainties, the states of the closed-loop FTC system are ultimately bounded instead of asymptotically convergent to zero. ∇

5. Simulations

The three-phase traction inverters in China Railway High-speed (CRH) system will be used to verify the proposed method in this paper, details of which are shown in fig. 1. The values of the physical parameters are given in table. 1 where ω_0 is the operating frequency when the traction motor works at the rated speed. As described in Zhang

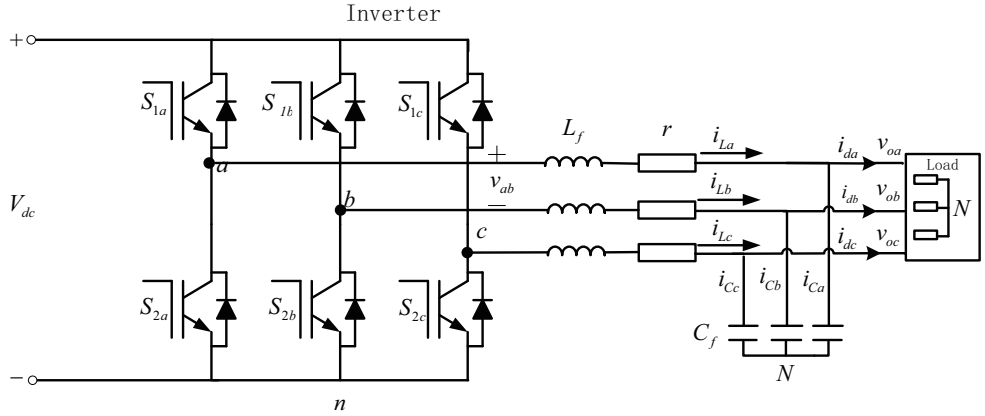

Figure 1. The topology of three-phase inverter.

Table 1. Parameters of the inverter.

Parameter	Value	Unit
r	0.144	Ω
L_f	1.417×10^{-3}	H
C_f	6000×10^{-6}	F
V_{dc}	3600	V
ω_0	200	rad/s

et al. (2017), for a constant operating frequency ω_0, the inverter can be modeled as a linear time-invariant system. Nevertheless, the running frequency varies with time in a limited range to regulate the rotation speed of the traction motors. Therefore, referring the dynamic model in Zhang et al. (2017), the inverter can be modeled as a LPV system given as follows:

$$\begin{aligned} \dot{x} &= Ax + \Delta A(\omega(t))x + B_0 u, \\ y &= Cx \end{aligned}$$

where $x = \mathrm{col}(x_1, x_2, x_3, x_4)$ with $x_1 = v_{od}$, $x_2 = v_{oq}$, $x_3 = i_{Ld}$, $x_4 = i_{Lq}$. These vectors $\mathrm{col}(v_{od}, v_{oq})$ and $\mathrm{col}(i_{Ld}, i_{Lq})$ represent positive-sequence and negative-sequence voltages and currents, respectively, which are obtained through the Park transformation and the Clark transformation for $\mathrm{col}(V_{oa}, V_{ob}, V_{oc})$ and $\mathrm{col}(i_{La}, i_{Lb}, i_{Lc})$ respectively. The variable $\omega(t)$ represents the offset frequency to ω_0, which belongs to the interval $[-100\mathrm{rad/s}, 100\mathrm{rad/s}]$, the control input u is determined by the switching signals S_{1a}, S_{1b}, S_{1c}, S_{2a}, S_{2b} and S_{2c} generated by IGBTs in fig. 1, the expression of u has been given in Zhang et al. (2017). In addition,

$$\begin{aligned} A &= \begin{bmatrix} 0 & \omega_0 & \frac{1}{C_f} & 0 \\ -\omega_0 & 0 & 0 & \frac{1}{C_f} \\ -\frac{1}{L_f} & 0 & -\frac{r}{L_f} & \omega_0 \\ 0 & -\frac{1}{L_f} & -\omega_0 & -\frac{r}{L_f} \end{bmatrix}, \ \Delta A(\omega) = \begin{bmatrix} 0 & \omega & 0 & 0 \\ -\omega & 0 & 0 & 0 \\ 0 & 0 & 0 & \omega \\ 0 & 0 & -\omega & 0 \end{bmatrix}, \\ C &= \begin{bmatrix} 0 & 0 & 1 & 0 \\ 0 & 0 & 0 & 1 \end{bmatrix}. \end{aligned}$$

It should be pointed out that the inverter dynamics given above is just for simulation purpose, which, actually, ignore the load currents. In addition, to verify the FTC method and to introduce actuator redundancy, a backup actuator u_3 for actuator u_1 is added in the model, which is reflected on the matrix B_0, described by

$$B_0 = \begin{bmatrix} 0 & 0 & 0 \\ 0 & 0 & 0 \\ \frac{V_{dc}}{L_f} & 0 & \frac{V_{dc}}{L_f} \\ 0 & \frac{V_{dc}}{L_f} & 0 \end{bmatrix}.$$

In the sequel, the specific values of the parameters used in the paper is calculated

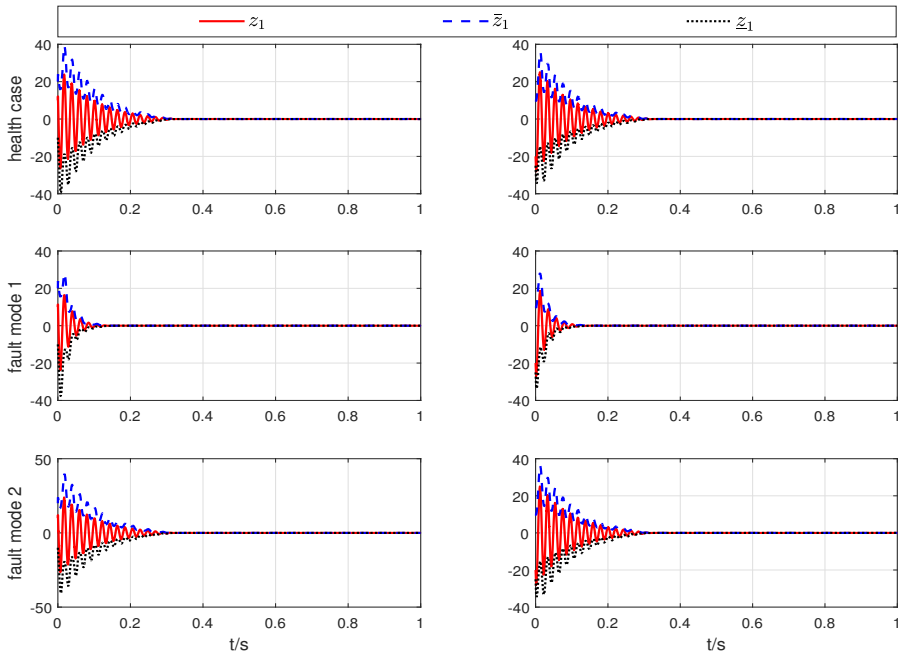

Figure 2. Time responses of $\bar{z}_1$, z_1 and $\underline{z}_1$.

and presented. Firstly, B_0 is decomposed by $B_0 = BE$ where

$$B = \begin{bmatrix} 0 & 0 \\ 0 & 0 \\ 254060 & 0 \\ 0 & 254060 \end{bmatrix}, \; E = \begin{bmatrix} 10 & 0 & 10 \\ 0 & 10 & 0 \end{bmatrix},$$

and then, system (8) can be obtained. Furthermore, the uncertainties $\Delta A_1(\omega)$ and $\Delta A_2(\omega)$ are obtained as

$$\Delta A_1(\omega) = \begin{bmatrix} 0 & \omega & 0 & 0 \\ -\omega & 0 & 0 & 0 \end{bmatrix}, \; \Delta A_2(\omega) = \begin{bmatrix} 0 & 0 & 0 & \omega \\ 0 & 0 & -\omega & 0 \end{bmatrix}.$$

By direct calculation, the triple $(A+\Delta A(\omega),\ B,\ C)$ is non-minimum phase. To satisfy Assumption 3.2, for $\omega \in [-100, 100]$,

$$\Delta A_1 = \begin{bmatrix} 0 & 100 & 0 & 0 \\ 100 & 0 & 0 & 0 \end{bmatrix}, \Delta A_2 = \begin{bmatrix} 0 & 0 & 0 & 100 \\ 0 & 0 & 100 & 0 \end{bmatrix}.$$

Consequently, γ_i, $i = 1, \cdots, 5$ used in (48)-(50) can be determined. For all $\hat{\rho} \in \Sigma$ satisfying Assumption 2.1, the scalar α in (45) is chosen as $\alpha = 0.1$ and γ_ρ is chosen as $\gamma_\rho = 0.5$. Then, the γ_0 can be obtained as $\gamma_0 = 1.4142$.

Now the matrix T satisfying Propositions 3.6 and 4.1 can be determined. Given $\epsilon_1 = 0.2$, $\epsilon_2 = 0.1$ and $\epsilon_3 = \epsilon_4 = 4$, using LMI toolbox, a feasible solution is obtained

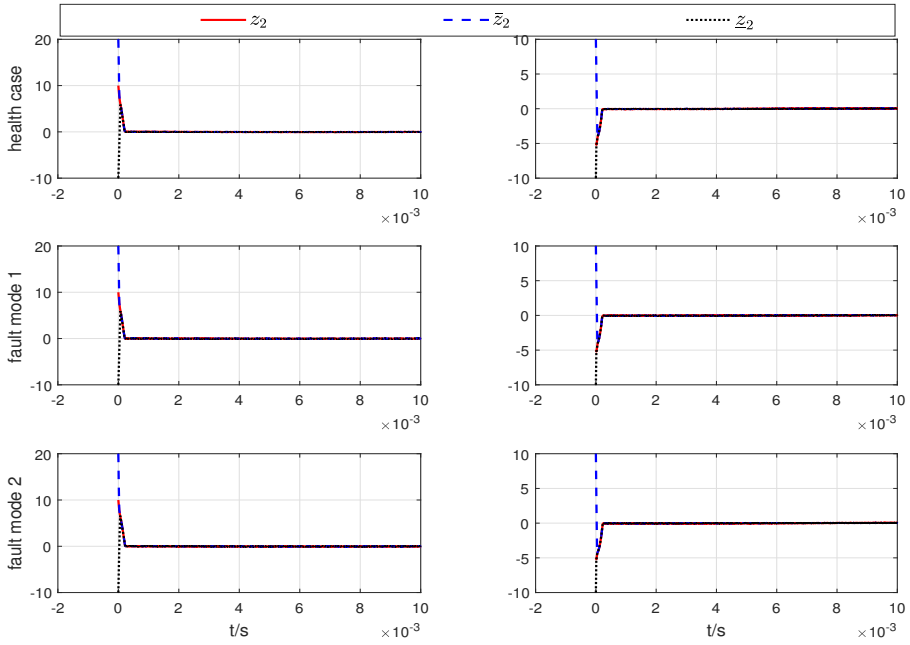

Figure 3. Time responses of $\bar{z}_2$, z_2 and $\underline{z}_2$.

by

$$T = \begin{bmatrix} -0.4372 & -0.0876 \\ 0.2911 & -0.4118 \end{bmatrix}.$$

In addition, the $\bar{A}_4$ used to determine L in Proposition 3.6 is chosen as $-100I_2$. Finally, the virtual control v is designed as (53) with v_l and v_n being determined by (54) and (55) respectively.

In the simulation, the healthy case $\rho = 0$, fault mode 1: $\rho = \text{diag}\{0.4, 0, 0\}$ and fault mode 2: $\rho = \text{diag}\{1, 0, 0\}$ are used. The time responses of the designed ISMO and the states z_1 and z_2 are shown in figs. 2 and 3. It can be seen that for all the simulated fault modes, the inequalities $\bar{z}_1 \leq z_1 \leq \underline{z}_1$ and $\bar{z}_2 \leq z_2 \leq \underline{z}_2$ hold all the time. Moreover, the simulation results show that z_1 in fig. 2 converges to zero asymptotically and z_2 in fig. 3 converges to zero in finite time for all the simulated fault modes. Therefore, the control objective is verified. In addition, the actual control efforts of the three actuators are shown in fig. 4. It can be observed that the control effort allocated to the first actuator $u(1)$ decreases while to the second one $u(3)$ increases as the loss of efficiency factor of $u(1)$ increases (which achieves the objective of the online CA scheme in this paper).

As stated in Krebs et al. (2016), for the above simulated inverter system, the uncertainties from current sensors and external uncertainties should be considered. In this case, to satisfy the extra condition $T \leq 0$ specified in Remark 10, the design parameter T is given as follows:

$$T = \begin{bmatrix} -0.2814 & -0.1638 \\ -0.1958 & -0.2510 \end{bmatrix}.$$

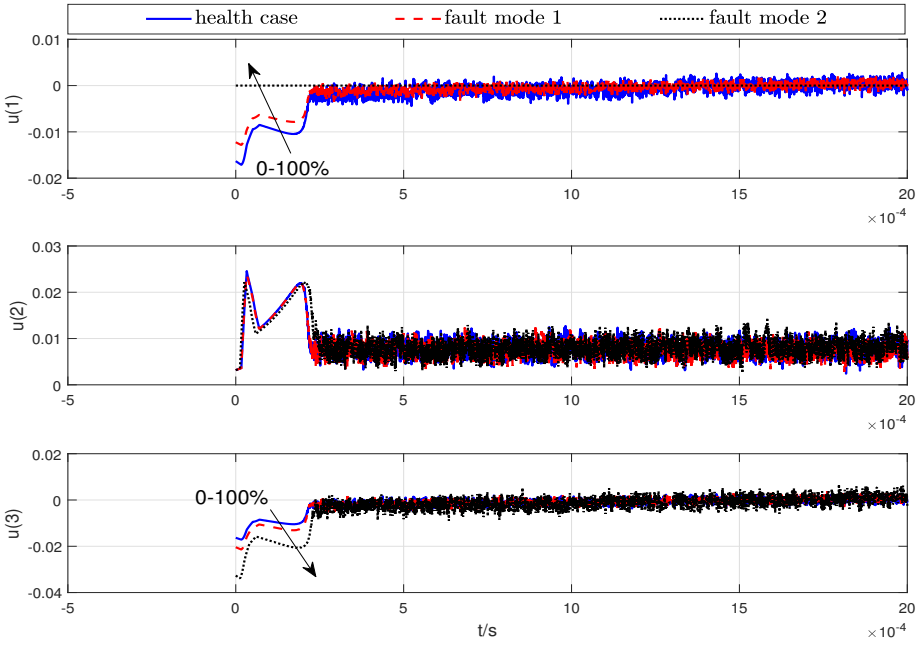

Figure 4. Time responses of u.

It is assumed that the measurement disturbance of the current sensor is $\pm 1\%$ of the real value. For simulation purposes, the disturbances of sensor measurements are given by $\xi = [\cos(10t+10),\ \sin(10t+5)]$. Then, Ξ is chosen as $\Xi = 2$. The simulation results are shown in figs. 5-7. it can be seen from figs. 5 and 6 that the designed ISMO can still provide interval estimates for the states z_1 and y. But comparing with figs. 2-4, the stability of the whole closed-loop FTC system is still able to be guaranteed even if input and output uncertainties appear in the system. However, due to these uncertainties, the developed FTC control law is not able to ensure all the states to converge to zero asymptotically. Fig. 7 illustrates the online CA results which show the same assignment trends for control efforts with fig. 4. From the above analysis, it is concluded that these simulation results verify the effectiveness of the developed FA method in this paper .

In the following, a comparison with the FTC scheme for LPV systems presented in Chen et al. (2017) will be shown. In Chen et al. (2017), the scheduling parameter vector θ and the matrix ρ related to the loss of efficiency factors are required to be known exactly. For simulation purposes, the fault mode is chosen as: $\rho = \text{diag}\{1, 0, 0\}$. The simulation results based on Chen et al. (2017) and this paper are shown in Figs. 8 and 9 respectively. It can be seen that due to more information used in Chen et al. (2017), the simulation results of Chen et al. (2017) are better than ones of this paper. However, it should be noted that Chen et al. (2017) needs to know the scheduling parameters and efficiency factors exactly. In addition, Chen et al. (2017) uses a state feedback FTC scheme while this paper proposes an output feedback FTC scheme which is more challenging.

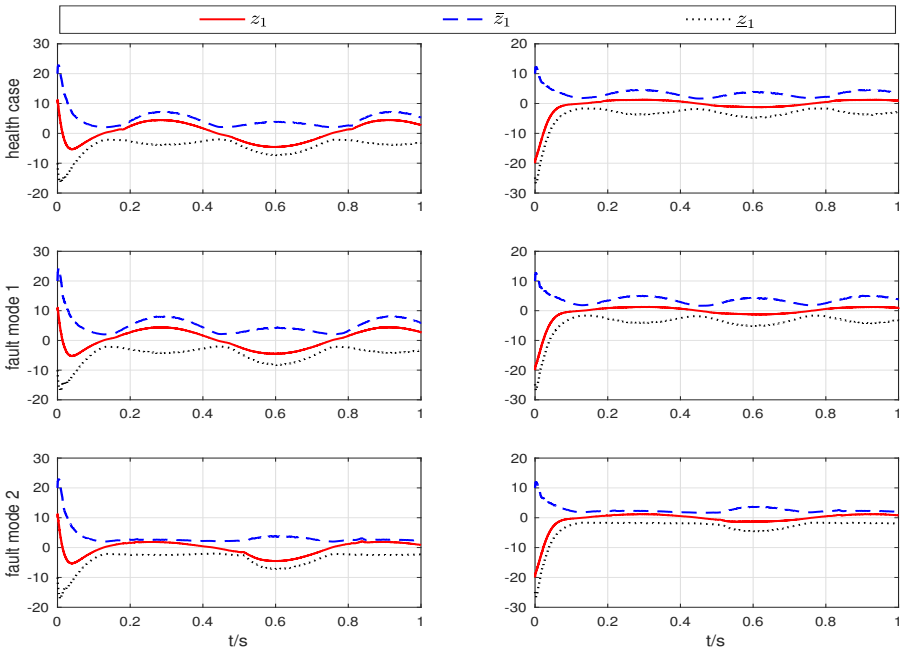

Figure 5. Time responses of $\bar{z}_1$, z_1 and $\underline{z}_1$.

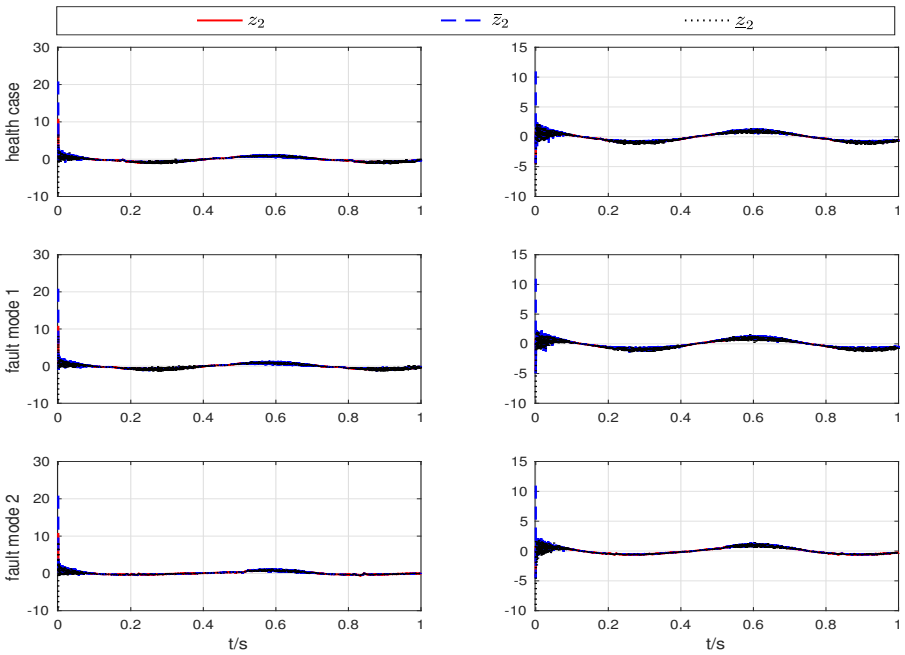

Figure 6. Time responses of $\bar{z}_2$, z_2 and $\underline{z}_2$.

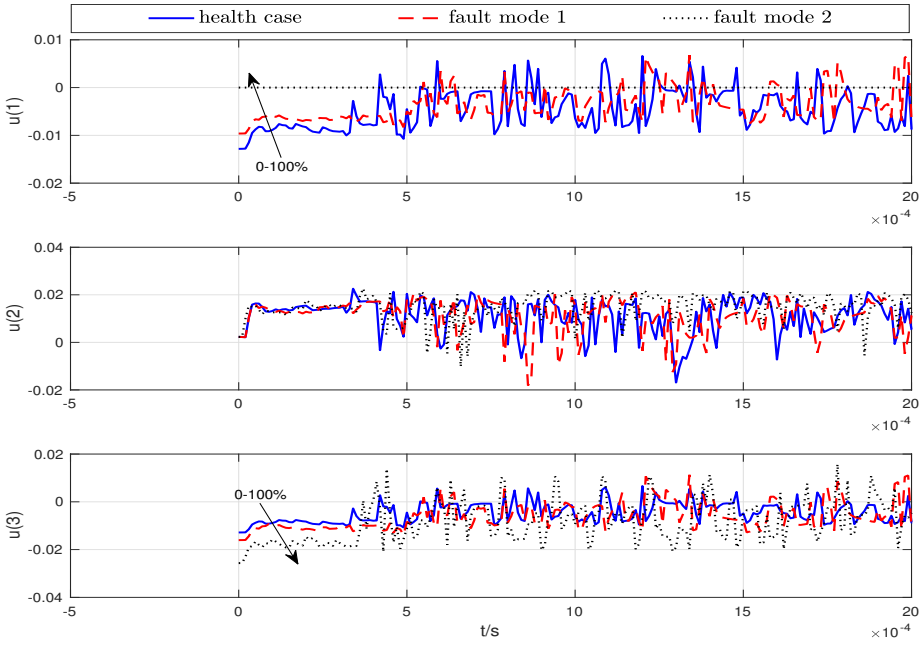

Figure 7. Time responses of u.

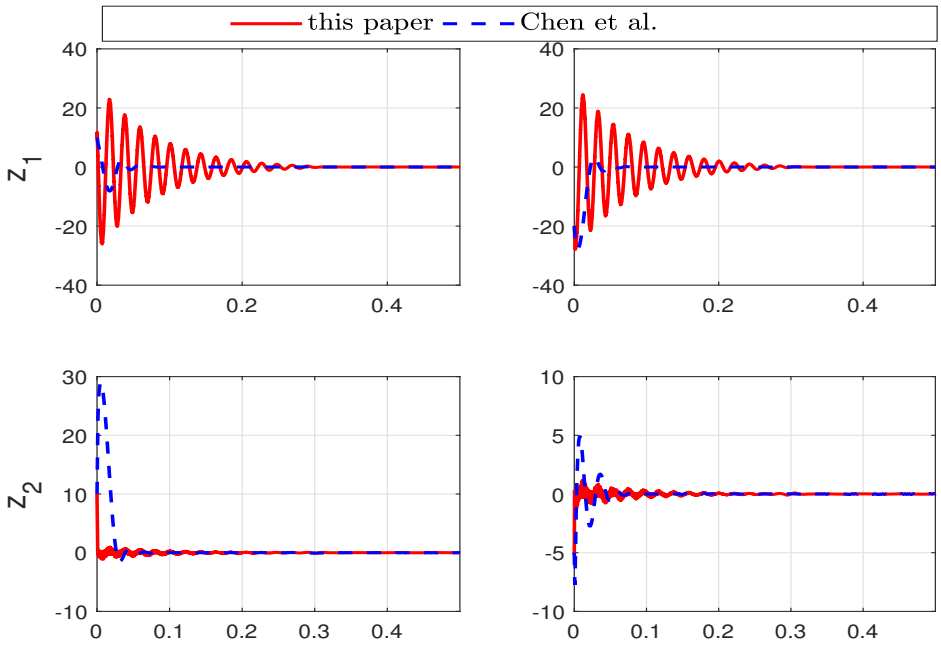

Figure 8. Time responses of z_1 and z_2.

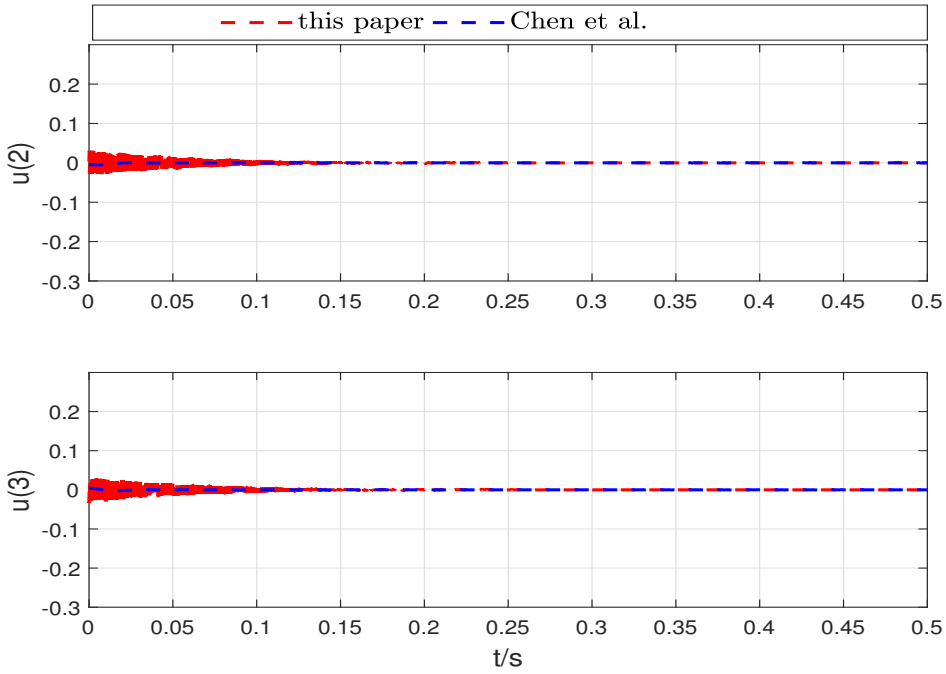

Figure 9. Time responses of u_2 and u_3.

6. Conclusions

This paper has proposed an ISMO based actuator FA framework for non-minimum phase LPV systems incorporating an online CA problem for faulty actuators. A coordinate transformation has been proposed to address the non-minimum phase problem. By combining interval observer and sliding mode observer techniques, an ISMO has been proposed based on the designed interval bounds for scheduling-parameter-related uncertainties and fault-related terms, which is able to generate tighter interval estimation than other interval observers. An ISMO based sliding mode FTC law with online CA scheme has also been designed such that the unmeasurable states of the original LPV system converge to zero asymptotically and the measurable outputs converged to zero in finite time, and the required control effort distributed among all actuators optimally to satisfy a prescribed performance simultaneously. Finally, a simulation example was presented to illustrate the effectiveness of the proposed FTC schemes.

Funding

This work was supported in part by the National Natural Science Foundation of China (Grants No 61903188, 61490703 and 61573180), the Natural Science Foundation of Jiangsu Province (Grants No BK20190403) and China Postdoctoral Science Foundation 2019M660114.

References

Alwi, H., & Edwards, C. (2008). Fault detection and fault-tolerant control of a civil aircraft using a sliding-mode-based scheme. *IEEE Transactions on Control Systems Technology*, *16*(3), 499–510.

Alwi, H., & Edwards, C. (2008). Fault tolerant control using sliding modes with online control allocation, *Automatica*, *44*(7), 1859–1866.

Alwi, H., & Edwards, C. (2014). Robust fault reconstruction for linear parameter varying systems using sliding mode observers, *International Journal of Robust and Nonlinear Control*, *24*(14), 1947–1968.

Alwi, H., Edwards, C., & Marcos, A. (2012). Fault reconstruction using a LPV sliding mode observer for a class of LPV systems, *Journal of the Franklin Institute*, *349*(2), 510–530.

Alwi, H., Edwards, C., & Tan, C. P. (2009). Sliding mode estimation schemes for incipient sensor faults, *Automatica*, *45*(7), 1679–1685.

Boskovic, J. D., & Mehra, R. K. (2010). A decentralized fault-tolerant control system for accommodation of failures in higher-order flight control actuators, *IEEE Transactions on Control Systems Technology*, *18*(5), 1103–1115.

Chebotarev, S., Efimov, D., Raïssi, T., & Zolghadri, A. (2015). Interval observers for continuous-time LPV systems with L_1/L_2 performance, *Automatica*, *58*, 82-89.

Chen, L., Alwi, H., & Edwards, C. (2017). Development and evaluation of an integral sliding mode fault-tolerant control scheme on the RECONFIGURE benchmark, *International Journal of Robust and Nonlinear Control*. Advance online publication. doi: 10.1002/rnc.3951.

Combastel, C. (2013). Stable interval observers in C for linear systems with time-varying input bounds. *IEEE Transactions on Automatic Control*, *58*(2), 481-487.

Edwards, C., & Spurgeon, S. (1998). *Sliding mode control: theory and applications*. London, UK: *CRC Press*.

Edwards, C., Yan, X. G., & Spurgeon, S. (2007). On the solvability of the constrained Lyapunov problem, *IEEE Transactions on Automatic Control*, *52*(10), 1982–1987.

Efimov, D., Fridman, L., Raïssi, T., Zolghadri, A., & Seydou, R. (2012). Interval estimation for LPV systems applying high order sliding mode techniques. *Automatica*, *48*(9), 2365–2371.

Efimov, D., & Raïssi, T. (2016). Design of interval observers for uncertain dynamical systems. *Automation and Remote Control*, *77*(2), 191–225.

Efimov, D., Raïssi, T., & Zolghadri, A. (2013). Control of nonlinear and LPV systems: interval observer-based framework, *IEEE Transactions on Automatic Control*, *58*(3), 773–778.

Fan, Q. Y., & Yang, G. H. (2017). Active complementary control for affine nonlinear control systems with actuator faults. *IEEE Transactions on Cybernetics*, *47*(11), 3542–3553.

Farina, L., & Rinaldi, S. (2011). *Positive linear systems: theory and applications*. New York, NY: *John Wiley & Sons, INC*.

Gao, Z. W., Cecati, C., & Ding, S. (2015). A survey of fault diagnosis and fault-tolerant techniques—Part I: Fault diagnosis with model-based and signal-based approaches. *IEEE Transactions on Industrial Electronics*, *62*(6), 3757–3767.

Gouzé, J. L., Rapaport, A., & Hadjsadok, M. Z. (2000). Interval observers for uncertain biological systems, *Ecological Modeling*, *133*(1-2), 45–56.

Hao, L. Y., & Yang, G. H. (2013). Robust fault tolerant control based on sliding mode method for uncertain linear systems with quantization, *Isa Transactions*, *52*(5), 600–610.

Jiang, B., Staroswiecki, M., & Cocquempot, V. (2006). Fault accommodation for nonlinear dynamic systems. *IEEE Transactions on Automatic Control*, *51*(9), 1578–1583.

Krebs, S., Lukas K., & Sören H. (2016, October). A new modelling and identification approach for guaranteed inclusion of a voltage source inverter's output voltages. *Proceedings of the 2016 International Conference on Control, Automation and Information Sciences (ICCAIS)*(pp. 112-119). Ansan, Korea: IEEE Aerospace and Electronic Systems Society.

Lamouchi, R., Raïssi, T., Amairi, M., & Aoun, M. (2018). Interval observer framework for fault-tolerant control of linear parameter-varying systems, *International Journal of Control*, *91*(3), 524–533.

Li, H. Y., Gao, H. J., Shi, P., & Zhao, X. D. (2014). Fault-tolerant control of markovian jump stochastic systems via the augmented sliding mode observer approach, *Automatica*, *50*(7), 1825–1834.

Mazenc, F., & Bernard, O. (2011). Interval observers for linear time-invariant systems with disturbances. *Automatica*, *47*(1), 140–147.

Oubabas, H., Djennoune, S., & Bettayeb, M. (2018). Interval sliding mode observer design for linear and nonlinear systems, *Journal of Process Control*, *61*, 12–22.

Polycarpou, M. M. (2001). Fault accommodation for nonlinear dynamic systems. *IEEE Transactions on Automatic Control*, *46*(5), 736–742.

Raïssi, T., Efimov, D., & Zolghadri, A. (2012). Interval state estimation for a class of nonlinear systems. *IEEE Transactions on Automatic Control*, *57*(1), 260-265.

Raïssi, T., Videau, G., & Zolghadri, A. (2010). Interval observer design for consistency checks of nonlinear continuous-time systems. *Automatica*, *46*(3), 518–527.

Rotondo, D., Nejjari, F., & Puig, V. (2014). A virtual actuator and sensor approach for fault tolerant control of LPV systems. *Journal of Process Control*, *24*(3), 203–222.

Shamma, J. S. (1998). *Analysis and design of gain scheduled control systems* (Doctoral dissertation). Retrieved from https://dspace.mit.edu/handle/1721.1/14551.

Shi, P., Liu, M., & Zhang, L. X. (2015). Fault-tolerant sliding-mode-observer synthesis of Markovian jump systems using quantized measurements, *IEEE Transactions on Industrial Electronics*, *62*(9), 5910–5918.

Sloth, C., Esbensen, T., & Stoustrup, J. (2010). Active and passive fault-tolerant LPV control of wind turbines. *Proceedings of the 2010 American Control Conference* (pp. 4640–4646). Baltimore, USA: IEEE Control System Society.

Tang, X. D., Tao, G., & Joshi, S. M. (2007). Adaptive actuator failure compensation for nonlinear MIMO systems with an aircraft control application. *Automatica*, *43*(11), 1869–1883.

Tao, G., Joshi, S. M., & Ma, X. L. (2001). Adaptive state feedback and tracking control of systems with actuator failures. *IEEE Transactions on Automatic Control*, *46*(1), 78–95.

Thabet, R. E. H., Raïssi, T., Combastel, C., Efimov, D., & Zolghadri, A. (2014). An effective method to interval observer design for time-varying systems. *Automatica*, *50*(10), 2677-2684.

Yan, X. G., & Edwards, C. (2007). Nonlinear robust fault reconstruction and estimation using a sliding mode observer, *Automatica*, *43*(9), 1605–1614.

Yang, G. H., & Ye, D. (2010). Reliable H_∞ control of linear systems with adaptive mechanism. *IEEE Transactions on Automatic Control*, *55*(1), 242–247.

Ye, D., Su, L., Wang, J. L., & Pan, Y. N. (2017). Adaptive reliable H_∞ optimization control for linear systems with time-varying actuator fault and delays, *IEEE Transactions on Systems, Man, and Cybernetics: Systems*, *47*(7), 1635–1643.

Ye, D., & Yang, G. H. (2006). Adaptive fault-tolerant tracking control against actuator faults with application to flight control. *IEEE Transactions on Automatic Control*, *14*(6), 1088–1096.

Zhang, K. K., Jiang, B., Yan, X. G., & Mao, Z. H. (2017). Adaptive robust fault-tolerant control for linear MIMO systems with unmatched uncertainties, *International Journal of Control*, *90*(10), 2253–2269.

Zhang, K. K., Jiang, B., Yan, X. G., & Mao, Z. H. (2017). Incipient sensor fault estimation and accommodation for inverter devices in electric railway traction systems, *International Journal of Adaptive Control and Signal Processing*, *31*(5), 785–804.

Zhang, K. K., Jiang, B., Yan, X. G., & Mao, Z. H. (2017). Incipient voltage sensor fault isolation for rectifier in railway electrical traction systems, *IEEE Transactions on Industrial Electronics*, *64*(8), 6763–6774.

Zhang, K. K., Jiang, B., Yan, X. G., Shen, J., & He, X. (2017). Incipient fault detection based on robust threshold generators: a sliding mode interval estimation approach, *IFAC paper online*, *50*(1), 5067–5072.

Zhang, Y. M., & Jiang, J. (2008). Bibliographical review on reconfigurable fault-tolerant control systems. *Annual Reviews in Control*, *32*(2), 229–252.

Zheng, G., Efimov, D., & Perruquetti, W. (2016). Design of interval observer for a class of uncertain unobservable nonlinear systems. *Automatica*, *63*, 167–174.